physica status solidi b
www.pss-b.com

Photo-Gain Effect in κ-Ga_2O_3 UV-C Photoresistors Induced by Trapping of Photogenerated Holes

Andrea Asteriti, Giovanni Verzellesi, Giovanna Sozzi, Andrea Baraldi, Piero Mazzolini, Abderrahim Moumen, Antonella Parisini, Maura Pavesi, Matteo Bosi, Roberto Mosca, Luca Seravalli, and Roberto Fornari*

The "photo-gain effect" amplifying the DC photocurrent of κ-Ga_2O_3 UV-C photoresistors is analyzed by means of 2D numerical simulations and linked to the capture of photogenerated holes by deep donor levels, probably associated with oxygen vacancies. The resulting ionization of the deep donors leads to an increase in the electron density, hence to enhanced conductivity under illumination.

1. Introduction

Ga_2O_3 is an ultrawide-bandgap semiconductor that enables the fabrication of solar-blind UV-C radiation detection devices without the need for filters to reject visible, UV-A and UV-B daylight.[1–3] Photoresistors based on undoped Ga_2O_3 epilayers represent a technologically simple detector configuration that may moreover benefit from the so-called "photo-gain effect", i.e., an enhanced photoresponse compared to that expected on the basis of the conductivity increase simply induced by the photogenerated electrons.[4] The trapping of photogenerated holes by deep levels has been suggested to be at the origin of this effect in Ga_2O_3 photodetectors.[5] It has also been correlated to high photocurrent and long decay time in amorphous-Ga_2O_3 optoelectronic synapses.[6] In this work, for the first time, we carried out 2D device simulations self-consistently accounting for charge transport, photogeneration of electron–hole pairs by the UV-C radiation, and the effect of deep-level traps, and quantitatively reproducing experimental results from κ-Ga_2O_3 UV-C photoresistors. The results support the idea of photo-gain as directly connected with hole trapping effects.

A. Asteriti, G. Verzellesi
Department of Sciences and Methods for Engineering
University of Modena and Reggio Emilia
Via Amendola 2, I-42122 Reggio Emilia, Italy
E-mail: giovanni.verzellesi@unimore.it

G. Sozzi
Department of Engineering and Architecture
University of Parma
Parco Area delle Scienze 181/a, I-43124 Parma, Italy

A. Baraldi, P. Mazzolini, A. Moumen, A. Parisini, M. Pavesi, R. Fornari
Department of Mathematical, Physical and Computer Sciences
University of Parma
Parco Area delle Scienze 7/A, I-43124 Parma, Italy

P. Mazzolini, M. Bosi, R. Mosca, L. Seravalli, R. Fornari
IMEM-CNR Institute of Materials for Electronics and Magnetism
I-43124 Parma, Italy

The ORCID identification number(s) for the author(s) of this article can be found under https://doi.org/10.1002/pssb.202400581.

DOI: 10.1002/pssb.202400581

2. Devices and Simulation Models

Devices at study are κ-Ga_2O_3 undoped photoresistors with 500 nm thickness, 4 mm width, and 2 mm electrode distance. More details on the fabrication process can be found in ref. [4]. 2D numerical device simulations were carried out with the Sentaurus Device tool that is part of the Synopsys TCAD suite.[7] Simulations self-consistently account for drift-diffusion charge transport, photogeneration effects, and deep-level traps.

The adopted charge-transport model more specifically consists of the Poisson's equation, relating the electric-potential distribution with the total space-charge density, and the two carrier-continuity equations, in which the current densities for electrons and holes are expressed as the sum of the drift and diffusion contributions.[8] The main parameters used for the simulations of κ-Ga_2O_3 can be found in ref. [9].

Optical generation is simulated by associating the intensity of the electromagnetic wave that is not reflected by the photoresistor surface to the photon flux entering the Ga_2O_3 layer. Photon absorption within the semiconductor layer is calculated by assuming a Poisson statistical distribution with average penetration depth $L = 1/\alpha$, where α is the absorption coefficient at the given wavelength, λ. The resulting photon flux exponentially decays along the penetration depth. Results shown below refer to illumination with light of wavelength $\lambda = 250$ nm. The optical generation rate at any point of the device reached by the photon flux is included into the carrier-continuity equations. **Figure 1** shows the 2D plot of the optical generation rate within the simulated Ga_2O_3 photoresistor by using $\alpha = 10^5\ cm^{-1}$.

Deep levels are modeled, with no quasistatic approximation, by a fully dynamic approach accounting for the Shockley–Read–Hall (SRH) detailed balance equation relating the level occupancy to the microscopic electron and hole emission and capture processes.[10,11] Deep-level contributions to both

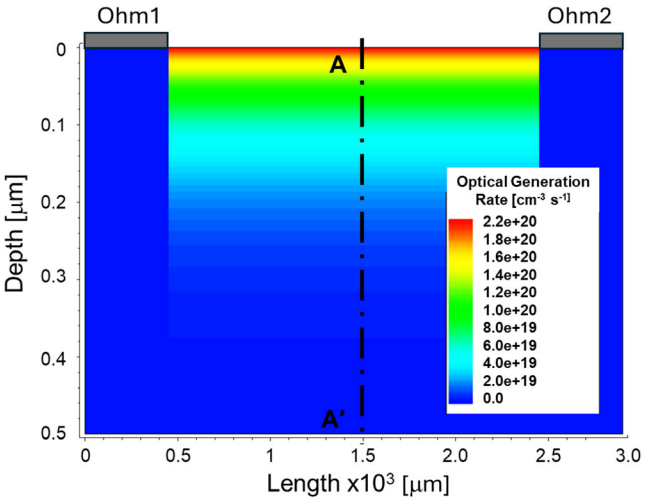

Figure 1. 2D contour plot of the optical generation rate within the simulated Ga_2O_3 photoresistor. Ohm1 and Ohm2 are the two ohmic contacts. Length and depth axis not to scale. A–A′ is the cutline along which the distributions of several internal quantities are plotted in Figure 4.

space-charge density and generation–recombination rate are accounted for, by adding appropriate terms to the Poisson's equation and the carrier-continuity equations, respectively.

The overall simulation model solved by the simulator is summarized in Appendix 1. Values of the main parameters adopted in the simulations (unless otherwise stated) are listed in **Table 1**.

Table 1. Values of main parameters adopted in the simulations.

Parameter	Value	Unit	Notes
Relative permittivity [ε]	10	–	–
Electron mobility [μ_n]	15	$cm^2\ (V\,s)^{-1}$	–
Hole mobility [μ_p]	0.001	$cm^2\ (V\,s)^{-1}$	–
Bandgap [E_G]	4.85	eV	–
Conduction band effective density of states [N_C]	3.7×10^{18}	cm^{-3}	–
Valence band effective density of states [N_V]	9.4×10^{20}	cm^{-3}	–
Electron lifetime [τ_n]	10^{-9}	s	–
Hole lifetime [τ_p]	10^{-9}	s	–
Unintentional n-type doping concentration [N_{UID}]	10^9	cm^{-3}	Uniform
Deep donor density [N_{DON}]	10^{16}	cm^{-3}	Uniform
Deep donor energy [E_{DON}]	1.4	eV	Referred to conduction band
Deep donor electron (hole) capture cross section [σ_n (σ_p)]	10^{-16} (10^{-16})	cm^2	–
Absorption coefficient (α) at $\lambda = 250$ nm	10^5	cm^{-1}	–

3. Results

Figure 2a shows the Arrhenius plot of the device conductance (G) measured in dark. As it can be noted, photoresistors exhibit in dark a thermally activated conductance (G) in the 400–600 K range. This can be ascribed to the thermal ionization of deep donor levels. The extracted activation energy is 0.69 eV. On the other hand, deep donors provide negligible contribution to the dark conductance from room temperature up to 400 K (i.e., for $1000/T$ ranging from 3.3 to 2.5).

In the simulated device, deep donor levels must be positioned at an energy (E_{DON}) of 1.3–1.4 eV from the Ga_2O_3 conduction band and have a density (N_{DON}) in the order of 10^{15}–$10^{16}\ cm^{-3}$, to fit the experimental results, both in terms of G value range and activation energy. Simulation results are shown in Figure 2b, for $N_{DON} = 10^{16}\ cm^{-3}$ and different E_{DON} values in the 1.2–1.6 eV range. The clear difference in G values that is observed for the same T but different energy-level E_{DON} of the deep donors is due to the different electron emission rate from traps to the conduction band that scales with E_{DON} as $\exp(-E_{DON}/k_BT)$ and the corresponding variation of the electron quasi-Fermi level E_{Fn} with respect to the conduction band edge. Similarly for G changes with temperature for a given E_{DON} value. To this respect, deep donor traps behave as incompletely ionized donor dopants, so that the electron quasi-Fermi level settles at a temperature-dependent position between E_C and the donor level E_{DON}. On the other hand, a net concentration of 10^8–$10^9\ cm^{-3}$ unintentional n-type shallow donors (N_{UID}) must be assumed, to get a simulated conductance consistent with the measured values below 400 K, where the contribution of deep donors to the conductance is negligible.

Shallow donors are the result of contamination and incorporation of hydrogen during the epitaxial deposition,[12–14] whereas the 1.3–1.4 eV donors are probably associated with oxygen vacancies.[13,15] Note that the value of 10^8–$10^9\ cm^{-3}$ for N_{UID} (assumed in the simulations to fit the G values measured in dark in the 300–400 K range) can be the net effect of a higher concentration of shallow donors, compensated by deep acceptors that have been shown to be present in Ga_2O_3[12] but are neglected in our simulations.

Figure 3a shows the measured and simulated DC photocurrent (I_{opt}) as a function of the applied voltage for an impinging 250 nm UV-C radiation of $1.8\ mW\ cm^{-2}$ intensity at room temperature. In the simulations, when deep donor are included with the same parameters assumed for dark simulations, i.e., $E_{DON} = 1.4$ eV and $N_{DON} = 10^{16}\ cm^{-3}$, the simulated I_{opt} (dots) is in very good agreement with experimental measurements (solid line). On the other hand, in agreement with ref. [5] if deep donors are not included in the simulations, photocurrent results are largely underestimated by simulations (squares).

Remarkedly, the I_{opt} obtained by simulations if deep-donor traps are neglected is a factor of 70 smaller than measured from actual devices, i.e., the existence of deep-donor levels is essential for theoretically explaining the experimental photoresponse of these Ga_2O_3 photoresistors. This is shown in Figure 3b, where simulated I_{opt} curves are reported for the two cases of $N_{DON} = 10^{16}$ and $0\ cm^{-3}$ in log scale.

Simulations explain the above results, as associated with the trapping of photogenerated holes by the deep donors. This is

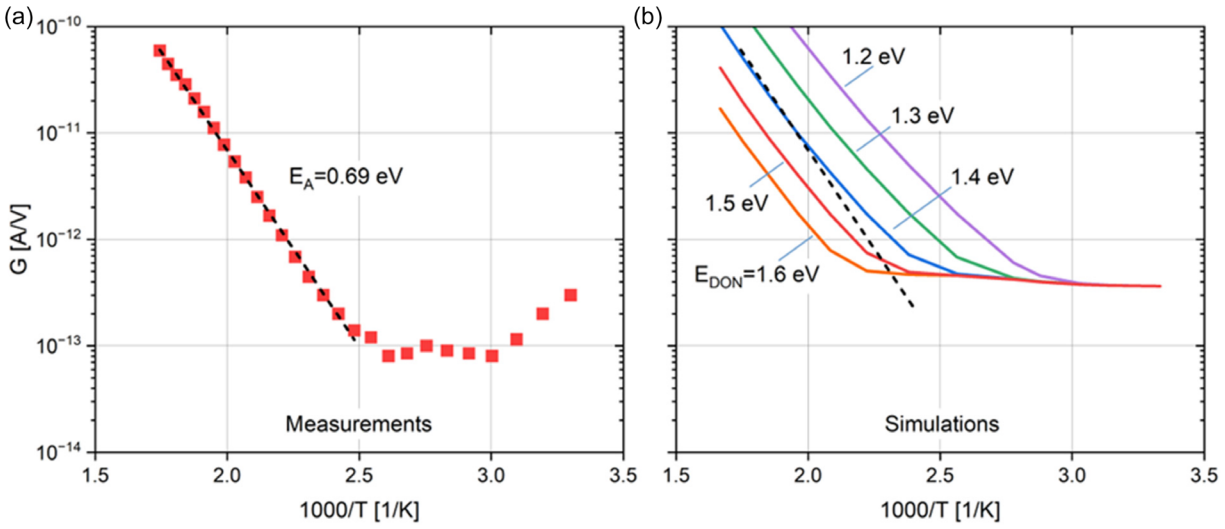

Figure 2. Arrhenius plot of a) measured and b) simulated dark conductance (G). A density of 10^{16} cm^{-3} deep donors at energy E_{DON} varying from 1.2 to 1.6 eV from the bottom of the κ-Ga_2O_3 conduction band is assumed in the simulations. The dashed line in (a) is the linear regression line from which an activation energy of 0.69 eV is determined. The same line is plotted in (b) as a reference for simulations.

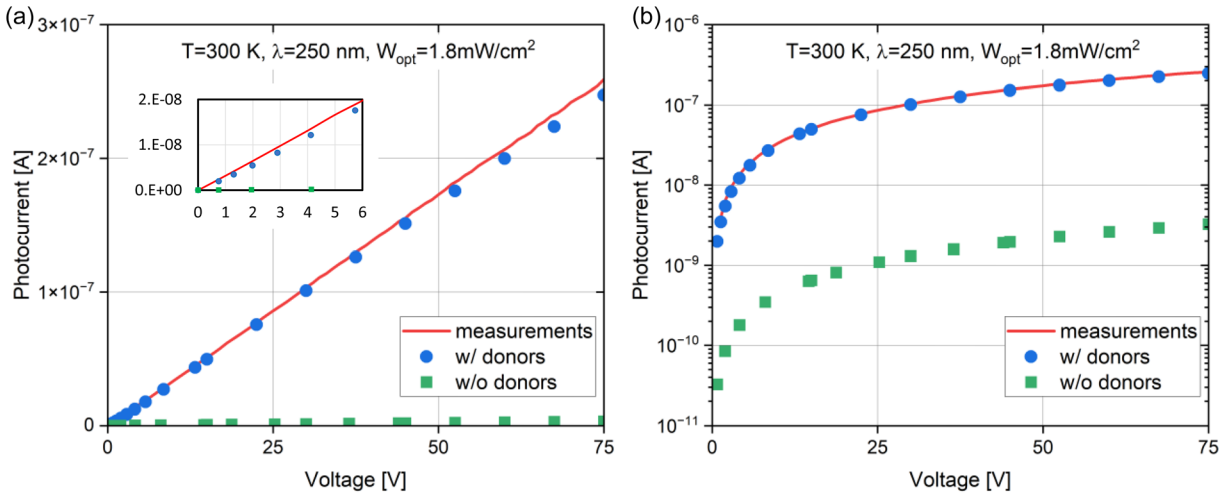

Figure 3. Measured (line) and simulated (symbols) DC photocurrent (I_{opt}) as a function of the applied voltage for an impinging UV-C radiation with 250 nm wavelength and 1.8 mW cm^{-2} intensity at room temperature. In the simulations, two cases are considered: one including deep donors ($E_{DON} = 1.4$ eV, $N_{DON} = 10^{16}$ cm^{-3}) and the other without deep donors. In a) the photocurrent scale is linear to illustrate the linearity of photoresistor response to the applied voltage. The inset is an enlarged plot of the low-voltage regime. The same curves are replotted in b) by using a logarithmic scale for the photocurrent to appreciate the presence of a photo-gain of about 70.

illustrated in detail by **Figure 4**a, showing 1D plots against device depth along a cutline in the middle of the gap between the two ohmic contacts (see line A–A′ in Figure 1) for the following quantities: (yellow line) hole trapped charge density, N_{DON}^+, (green line) hole density, p, (red line) electron density, n, and (blue line) net space-charge density, $\rho = N_{DON}^+ - n + p$. Illumination and deep donor parameters are the same of Figure 3, while the applied voltage is 75 V at room temperature (RT). As it can be noted, $n \gg$ p (besides being much larger than N_{UID}). This is due to the "photo-gain effect," i.e., the positive charge associated with trapped holes calls for the injection of extra electrons into the device. The deep donor density is assumed uniform within the Ga_2O_3 layer and equal to the value $N_{DON} = 10^{16}$ cm^{-3}. N_{DON}^+ is the density of positively ionized traps, that is, the fraction of N_{DON} that actually trapped holes. N_{DON}^+ is not uniform but a function of depth because photogeneration of (free) holes, by photons of energy larger than the bandgap, decreases exponentially with depth and hole capture probability at any given point of the semiconductor is proportional to the density of available holes in that point.[10] N_{DON}^+ is two orders of magnitude larger than free hole density, i.e., most of photogenerated holes are trapped by the deep

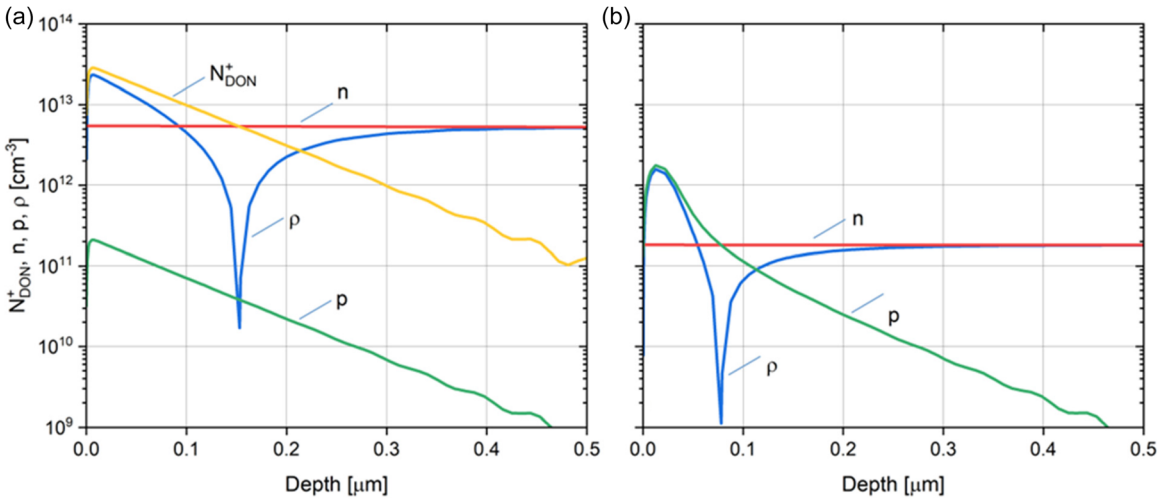

Figure 4. 1D plot along a cutline in the middle of the gap between the two ohmic contacts (see line A–A′ in Figure 1) of the following quantities: (yellow line) hole trapped charge density, $N_{DON}{}^{+}$, (green line) hole density, p, (red line) electron density, n, and (blue line) net space-charge density, $\rho = N_{DON}{}^{+} - n + p$. Illumination parameters are the same of Figure 3 and applied voltage is 75 V at RT. Deep donor density is $N_{DON} = 10^{16}\,cm^{-3}$ and 0 in a) and b), respectively.

donors. Moreover, ρ is dominated by $N_{DON}{}^{+}$ close to the surface, where optical generation is maximum, whereas it tends to n toward the bottom of the Ga_2O_3 layer, where optical generation is negligible. On the other hand, ρ is small around its sign inversion point at about 0.16 μm where $N_{DON}{}^{+} = n$. Overall charge neutrality is of course conserved as the integral of ρ is null. In other words, the 1.4 eV deep donors are ionized by trapping of photogenerated holes, thus amplifying the photoresistor conductivity compared to that related to the UID concentration. This only occurs under illumination, whereas, in the dark, the deep donors require high temperatures to be ionized (see Figure 2). In this case, customary thermal electron emission to the conduction band is the ionization mechanism. In both conditions, responsible deep levels need to be donor-like in order to provide a source for positive fixed charges when ionized.

For comparison, the same quantities are plotted in Figure 4b for the case $N_{DON} = 0$, i.e., without deep donors. As it can be seen, without deep donors, there is no photo-gain effect, so that n is much smaller than in Figure 4a, i.e., when deep donors are included in the modeling. Moreover, only the density of photogenerated electrons (n) and holes (p) contributes to the ρ. In principle, a small hole mobility compared to the electron one can lead to a photo-gain effect even in the absence of hole trapping. However, we verified that this effect is too small (less than a 2× photo-gain even for a six order-of-magnitude change in hole mobility) to explain photocurrent values obtained in the devices under study.

As it can be noted in both Figure 4a,b, the electron and hole density distributions have very different shapes, even if electron and holes are photogenerated in pairs. This is an effect of the large difference in electron and hole mobility and therefore diffusivity. Diffusion makes the electron density distribution almost uniform. The hole density distribution, on the contrary, follows the photogeneration rate profile (i.e., exponential dependence versus depth) owing to the very small hole diffusivity.

4. Conclusion

The "photo-gain effect", known to enhance the DC photoresponse of κ-Ga_2O_3 UV-C photodetectors and previously attributed to photogenerated hole trapping, has, for the first time, been verified by means of 2D numerical device simulations. Simulations quantitatively reproduce both dark conductance and DC photocurrent in undoped κ-Ga_2O_3 photoresistors while providing a detailed description of the underlying physics. Deep donors, which are probably related to oxygen vacancies, are shown to be the most plausible cause for the observed, high-temperature thermally activated conductance in dark, as well as for the photo-gain effect under UV-C illumination. The latter can be induced by the deep-donor trapping of photogenerated holes and the resulting increase in electron density and device conductivity. Although this simulation was carried out for a specific device based on high-resistivity epitaxial κ-Ga_2O_3, its validity is general. Therefore, it may be applied to a wide range of UV photoresistors, based on other Ga_2O_3 polymorphs or other wide-bandgap materials, whenever the photocurrent exceeds the one expected considering the photon flux.

Appendix

The charge-transport model solved by the simulator within the Ga_2O_3 layer consists of the Poisson's Equation (A1), relating the electric-potential distribution with the total space-charge density, and the two carrier-continuity Equation (A2) and (A3), describing charge conservation.[8]

$$\nabla\cdot(\varepsilon\nabla\varphi) = -q(p - n + N_{UID} + N_{DON}{}^{+}) \tag{A1}$$

$$\frac{\partial n}{\partial t} = \frac{1}{q}\nabla\cdot J_n - (U_{n,th} - G_{opt}) \tag{A2}$$

$$\frac{\partial p}{\partial t} = -\frac{1}{q}\nabla \cdot J_p - (U_{p,\mathrm{th}} - G_{\mathrm{opt}}) \tag{A3}$$

In Equation (A1)–(A3), φ is the electrostatic potential, ε is the electrical permittivity, q is the elementary electronic charge, n is the electron density, p is the hole density, N_{UID} is the concentration of unintentional shallow donors (assumed all completely ionized), $N_{\mathrm{DON}}{}^{+}$ is the concentration of ionized deep donor traps, J_n is the electron current density, J_p is the hole current density, $U_{n,\mathrm{th}}$ is the net thermal recombination rate for electrons, $U_{p,\mathrm{th}}$ is the net thermal recombination rate for holes, and G_{opt} is the optical generation rate (number of electron-hole pairs photogenerated per unit volume and time).

The current densities J_n and J_p are expressed as the sum of drift and diffusion terms through Equation (A4) and (A5).

$$J_n = -q\mu_n n\nabla\varphi + qD_n\nabla n \tag{A4}$$

$$J_p = -q\mu_p p\nabla\varphi - qD_p\nabla p \tag{A5}$$

where μ_n and μ_p are the electron and hole mobilities, whereas D_n and D_p are the electron and hole diffusivities, related to mobilities through the Einstein's relations:

$$D_n = \frac{k_B T_L}{q}\mu_n, \quad D_p = \frac{k_B T_L}{q}\mu_p \tag{A6}$$

k_{B} and T_{L} being the Boltzmann constant and the lattice temperature, respectively.

Photon absorption within the Ga_2O_3 layer is calculated by assuming a Poisson statistical distribution with average penetration depth $L = 1/\alpha$, where α is the absorption coefficient at the given wavelength. This leads to the following G_{opt} expression to be used in Equation (A2) and (A3)

$$G_{\mathrm{opt}} = \alpha\Phi_0 \exp(-\alpha\xi) \tag{A7}$$

where Φ_0 is photon flux at the Ga_2O_3 surface exposed to the UV-C illumination and ξ is the distance from the surface along the photon penetration path.

Donor traps are modeled by means of the SRH detailed balance Equation (A8), relating the level occupancy to the microscopic electron and hole emission and capture processes.[10,11]

$$\frac{\partial(N_{\mathrm{DON}} - N_{\mathrm{DON}}{}^{+})}{\partial t} = c_n N_{\mathrm{DON}}{}^{+} n - e_n(N_{\mathrm{DON}} - N_{\mathrm{DON}}{}^{+}) - c_p(N_{\mathrm{DON}} - N_{\mathrm{DON}}{}^{+})p + e_p N_{\mathrm{DON}}{}^{+} \tag{A8}$$

In Equation (A8), c_n and c_p are the electron and hole capture probability, e_n and e_p are the electron and hole emission probability, whereas N_{DON}, $N_{\mathrm{DON}}{}^{+}$, $(N_{\mathrm{DON}} - N_{\mathrm{DON}}{}^{+})$ are the deep donor, the ionized deep donor, and the neutral deep donor concentrations, respectively.

$c_{n(p)}$ is linked to the trap capture cross sections $\sigma_{n(p)}$ through the relationships $c_n = \sigma_n v_{\mathrm{th}}^{n}$ and $c_p = \sigma_p v_{\mathrm{th}}^{p}$, where $v_{\mathrm{th}}^{n(p)}$ is the electron(hole) thermal velocity. e_n and e_p are instead expressed as

$$e_n = c_n N_{\mathrm{C}} \exp\left[-\frac{E_{\mathrm{DON}}}{k_{\mathrm{B}} T_{\mathrm{L}}}\right] \tag{A9}$$

$$e_p = c_p N_{\mathrm{V}} \exp\left[-\frac{E_{\mathrm{G}} - E_{\mathrm{DON}}}{k_{\mathrm{B}} T_{\mathrm{L}}}\right] \tag{A10}$$

where E_{DON} is the trap energy offset from the conduction band edge, E_{G} is the bandgap (so that $E_{\mathrm{G}} - E_{\mathrm{DON}}$ is the trap energy offset from the valence band edge), whereas N_{C} and N_{V} are the effective density of states for conduction and valence band.

Equation (A1)–(A10) are discretized and self-consistently solved by the simulator over the 2D device cross section (see Figure 1).

Acknowledgements

This work was carried out in the frame of the project UV-C sensors based on gallium oxide (USE GAO, code no. 2022A4AN2F), PRIN2022, PNRR-M4C2-I1.1-MUR funded by NextGenerationEU.

Open access publishing facilitated by Universita degli Studi di Modena e Reggio Emilia, as part of the Wiley - CRUI-CARE agreement.

Conflict of Interest

The authors declare no conflict of interest.

Author Contributions

Andrea Asteriti: conceptualization (equal); data curation (equal); investigation (equal); validation (equal); writing—review and editing (equal). **Giovanni Verzellesi**: conceptualization (equal); funding acquisition (equal); investigation (equal); methodology (equal); software (equal); supervision (equal); validation (equal); writing—original draft (lead). **Giovanna Sozzi**: conceptualization (equal); investigation (equal); methodology (equal); supervision (equal). **Andrea Baraldi**: conceptualization (equal); methodology (equal). **Piero Mazzolini**: conceptualization (equal); methodology (equal). **Abderrahim Moumen**: conceptualization (equal); methodology (equal). **Antonella Parisini**: conceptualization (equal); methodology (equal); supervision (supporting); writing—review and editing (equal). **Maura Pavesi**: conceptualization (equal); data curation (equal); investigation (equal); methodology (equal); writing—review and editing (equal). **Matteo Bosi**: conceptualization (equal); funding acquisition (equal); supervision (supporting); validation (equal); writing—review and editing (equal). **Roberto Mosca**: conceptualization (equal); methodology (equal). **Luca Seravalli**: conceptualization (equal); methodology (equal). **Roberto Fornari**: funding acquisition (lead); investigation (equal); methodology (equal); project administration (lead); supervision (equal); validation (equal); writing—review and editing (lead).

Data Availability Statement

The data that support the findings of this study are available from the corresponding author upon reasonable request.

Keywords

deep traps, gallium oxide, photodetectors, photo-gain

Received: October 29, 2024
Revised: January 9, 2025
Published online:

[1] Y. Xu, X. Chen, Y. Zhang, F. Ren, S. Gu, J. Ye, *IEEE Electron Device Lett.* **2020**, *41*, 997.

[2] J. Bae, D.-W. Jeon, J.-H. Park, J. Kim, *J. Vac. Sci. Technol., A* **2021**, *39*, 033410
[3] S. Kim, Y. Yoon, D. Seo, J.-H. Park, D.-W. Jeon, W. S. Hwang, M. Shin, *APL Mater.* **2023**, *11*, 061107.
[4] M. Pavesi, F. Fabbri, F. Boschi, G. Piacentini, A. Baraldi, M. Bosi, E. Gombia, A. Parisini, R. Fornari, *Mater. Chem. Phys.* **2018**, *205*, 502.
[5] C. Borelli, A. Bosio, A. Parisini, M. Pavesi, S. Vantaggio, R. Fornari, *Mater. Sci. Eng., B* **2022**, *286*, 116056.
[6] R. Zhu, H. Liang, S. Hu, Y. Wang, Z. Mei, *Adv. Electron. Mater.* **2022**, *8*, 2100741.
[7] https://www.synopsys.com/manufacturing/tcad/device-simulation.html **2025**.
[8] S. Sze, *Physics of Semiconductor Devices*, 2nd ed., Wiley, New York **1981**.
[9] P. R. Kalvani, A. Parisini, G. Sozzi, C. Borelli, P. Mazzolini, O. Bierwagen, S. Vantaggio, K. Egbo, M. Bosi, L. Seravalli, R. Fornari, *ACS Appl. Mater. Interfaces* **2023**, *15*, 45997.
[10] W. Shockley, W. Read, *Phys. Rev.* **1952**, *87*, 835.
[11] R. Hall, *Phys. Rev.* **1952**, *87*, 387.
[12] A. Parisini, A. Bosio, H. J. von Bardeleben, J. Jimenez, S. Dadgostar, M. Pavesi, A. Baraldi, S. Vantaggio, R. Fornari, *Mater. Sci. Semicon. Process* **2022**, *138*, 106307.
[13] P. Mazzolini, J. B. Varley, A. Parisini, A. Sacchi, M. Pavesi, A. Bosio, M. Bosi, L. Seravalli, B. M. Janzen, M. N. Marggraf, N. Bernhardt, M. R. Wagner, A. Ardenghi, O. Bierwagen, A. Falkenstein, J. Kler, R. A. De Souza, M. Martin, F. Mezzadri, C. Borelli, R. Fornari, *Mater. Today Phys.* **2024**, *45*, 101463.
[14] A. Y. Polyakov, E. B. Yakimov, V. I. Nikolaev, A. I. Pechnikov, A. V. Miakonkikh, A. Azarov, I.-H. Lee, A. A. Vasilev, A. I. Kochkova, I. V. Shchemerov, *Crystals* **2023**, *13*, 1400.
[15] S. Li, J. Yue, X. Ji, C. Lu, Z. Yan, P. Li, D. Guo, Z. Wu, W. Tang, *J. Mater. Chem. C*, **2021**, *9*, 5437.